Communications on Applied Nonlinear Analysis
ISSN: 1074-133X
Vol 31 No. 7s (2024)

Heat Transfer in A Non-Uniform Channel Under the Action of Peristalsis

Suresh Chelikani[1], Murty V R K [2]

[1]Department of Mathematics, Rajiv Gandhi University of Knowledge Technologies, Nuzvid 521202, India.

[2]Department of Mathematics and Statistics, School of Applied Science and Humanities, Vignan's Foundation for Science, Technology and Research, Guntur 522213, India.

Email: chelikanisuresh23@gmail.com, vadapalli.radhakrishna@gmail.com.

Article History:

Received: *01-06-2024*

Revised: *03-07-2024*

Accepted: *29-07-2024*

Abstract:

An analytical study has been carried out on the heat transfer for motion of a viscous, incompressible Newtonian fluid. Sinusoidal waves travel through a two-dimensional, non-uniform channel. The governing equations are simplified under the assumption of long wave length and low Reynolds number. In this connection, the appropriate variables have been used to obtain the system of ordinary differential equations. The perturbation approach is used to achieve a numerical solution in terms of the small parameter 'd/λ'. The graphic results are obtained using MATLAB. Temperature and heat transfer have been analyzed, and the numerical findings are provided. The impact of relevant factors (Prandtl number, Eckert's number, Reynolds number, wall slope parameter, and amplitude ratio) on temperature has been examined.

Keywords: peristalsis, heat transfer, non-uniformity, temperature.

1. Introduction

In fluid dynamics, peristalsis refers to the generation of waves or propagating disturbances that occur within a fluid medium. Although this phenomenon shares its name with the biological process, the underlying principles are remarkably similar.

Peristaltic fluid dynamics have found numerous applications in a wide range of fields, including engineering, medicine, nuclear industries, and biology. Engineers utilize this concept to design and optimize various fluid transport systems, such as pumps, pipelines, and mixers. In medicine, peristaltic pumps are often used for drug delivery, intravenous fluid administration, and other medical applications requiring precise and controlled fluid movement. It is used to reduce the mechanical strain and accurate dosing in biomechanical instruments like dialysis machines, open-heart bypass pump machines, and artificial lungs and tissues. In the nuclear industry, peristalsis is used for contamination-free pumping. In biology, peristalsis is explored to understand the flow dynamics of bodily fluids, such as blood flow in blood vessels and the movement of cerebrospinal fluid within the spinal cord.

Peristalsis has been studied by a number of researchers for a variety of physiological and mechanical problems. Srinivas ANS investigated the peristaltic process for a Casson fluid with elastic tubes and permeable walls [4]. Kavitha A investigated the behavior of a two-fluid flow with the Jeffrey fluid in contact with a Newtonian fluid [5]. Prasad KV investigated how the transverse magnetic field affected the flow and the effects of temperature and species concentration [6]. Heat transfer for Rabinowitsch fluid under the influence of compliant walls was studied by Saravana [7]. Devaki P has also done

research on how wall characteristics affect the peristalsis of the Casson fluid model [9]. Divya BB investigated the physics of mass and heat transmission in the Casson fluid with varying viscosity [10]. The temperature distribution of a nanofluid under a magnetic field was studied by Alhazmi [11]. The present study is about how peristalsis and heat transfer interact when a viscous, incompressible Newtonian fluid moves through a two-dimensional, non-uniform channel. A mathematical model is provided here. Analytical solutions for velocity and temperature have been derived after the momentum and energy equations were linearized using the long wavelength approximation.

The structure of this article is as follows: The problem model is found in Section 2. Section 3 provides a detailed description of the chosen method. Section 4 presents the study results and their interpretation, as well as practical applications and prospective directions for future research.

2. Mathematical Model

Figure 1 depicts the flow of a viscous, incompressible Newtonian fluid through a two-dimensional, irregular conduit with flexible walls. It is opted to use the Cartesian coordinate system with the horizontal axis aligned with the channel's centre line and the direction in which waves travel along the walls. The wall channel's geometry is provided by

$$H(x,t) = d(x) + a\cos\frac{2\pi}{\lambda}(x - ct) \quad (1)$$

, where

$$d(x) = d + k'x \; (k' << 1).$$

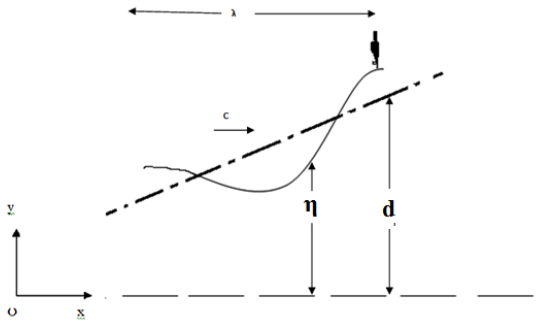

Figure 1. Flow geometry

The flow is governed by the equations

Momentum equation:

$$u_t + uu_x + vu_y = \frac{-1}{\rho}p_x + v\nabla^2 u \; . \quad (2)$$

$$v_t + uv_x + vv_y = \frac{-1}{\rho}p_y + v\nabla^2 v. \quad (3)$$

Continuity equation:

$$u_x + v_y = 0. \quad (4)$$

Energy equation:

$$6(T_t + uT_x + vT_y) = \frac{K}{\rho}\nabla^2 T + v\varphi \quad (5)$$

, where

$$\phi = 2\left[(u_x)^2 + (v_y)^2\right] + \left(v_x + u_y\right)^2. \quad (6)$$

The boundary conditions are:

$$\left.\begin{matrix} u = 0 \\ v = H_t \\ T = T_0 \end{matrix}\right| \quad on\ y = \pm H. \quad (7)$$

Remove the pressure term from equations (2) and (3) and taking stream function 'ψ' as

$$u = \psi_y, v = -\psi_x \quad (8)$$

and introducing the non-dimensional variables

$$x' = \frac{x}{\lambda}, y' = \frac{y}{d}, t' = \frac{c}{\lambda}t, \psi' = \frac{\psi}{cd}, \theta = \frac{T-T_0}{T_0} \quad (9)$$

in Eqns. (1),(2),(3), (5),(6) and (7), we get (after dropping the primes),

$$\nabla^2\psi_t + \psi_y\nabla^2\psi_x - \psi_x\nabla^2\psi_y = \frac{1}{\delta R}\nabla^4\psi. \quad (10)$$

$$R\delta\left[\theta_t + \psi_y\theta_x - \psi_x\theta_y\right] = \frac{1}{P}\nabla^2\theta + E\left[4\delta^2\left(\psi_{xy}\right)^2 + \left(\psi_{yy} - \delta^2\psi_{xx}\right)^2\right]. \quad (11)$$

$$\left.\begin{matrix} \psi_y = 0 \\ \psi_x = \mp 2\pi\epsilon sin2\pi(x-t) \\ \theta = 0 \end{matrix}\right| on\ y = \pm\eta \quad (12)$$

, where

$$\eta(x,t) = 1 + Kx + \epsilon\cos 2\pi(x-t) \quad (13)$$

$$\eta(x,t) = \frac{H(x,t)}{d}$$

$$\nabla^2 = \left(\delta^2\frac{\partial^2}{\partial x^2} + \frac{\partial^2}{\partial y^2}\right) \quad (14)$$

$$R = \frac{cd}{v} \qquad E = \frac{c^2}{6T_0}$$

$$P = \frac{\rho v 6}{k} \qquad \epsilon = \frac{a}{d}$$

$$\delta = \frac{d}{\lambda} \qquad K = \frac{\lambda k'}{d}. \quad (15)$$

3. Solutions

In terms of the small parameter 'δ', we look for perturbation solutions as follows:

$$g = g_0 + \delta g_1 + \delta^2 g_2 + \cdots \quad (16)$$

, where 'g' stands for any flow-related variable.

The Eqn (16) is substituted for Eqns (10) and (11), and the resulting equations are solved under the appropriate boundary conditions (12) by gathering coefficients of various powers of 'δ' (up to first order) to get

$\psi = \psi_0 + \delta\psi_1$ (17)

$\theta = \theta_0 + \delta\theta_1$ (18)

, where

$$\psi_0 = A_3 y^3 + A_1 y \quad (19)$$

$$\psi_1 = R[D_1 y^7 + D_2 y^5 + k_3 y^3 + k_1 y] \quad (20)$$

$$\theta_0 = -PE[3A_3^2 y^4 + c_1] \quad (21)$$

$$\theta_1 = PER\left[H_1 \frac{y^8}{56} + H_2 \frac{y^6}{30} + H_3 \frac{y^4}{12} + H_4 \frac{y^2}{2} + P_1\right] \quad (22)$$

$$A_3 = \frac{c_0 - \frac{1}{2}\epsilon cos2\pi(x-t)}{\eta^3}$$

$$A_1 = -3A_3\eta^2$$

$$D_1 = \frac{A_3 A_{3x}}{70}$$

$$D_2 = \frac{1}{20}(A_{3t} + A_1 A_{3x} - A_3 A_{1x})$$

$$c_1 = -3A_3^2\eta^4$$

The other constants are not given, as they are too lengthy. Z is given by

$$Z = Z_0 + \delta Z_1 \quad (23)$$

Where,

$$Z_0 = \eta_x \theta_{0y} \quad (24)$$

$$Z_1 = \theta_{0x} + \eta_x \theta_{1y} \quad (25)$$

4. Results And Discussion

Equations (18) and (23) provide the equation for temperature and the coefficient of heat transfer. Equation (18) has been numerically assessed to explicitly show how different parameters affect temperature, and the results are shown in figs. 2–7. Backflow does not happen for low values of K.

Zien and Ostrach [2] demonstrate that the constant of integration, c_0, emerges during the integration of the momentum equation. In order to plot all the graphs, its value is set to '-0.15' in this instance. Additionally, in figures 2–5 and 7, the value of 'K' is assumed to be 0.1, indicating that the channel is divergent in nature.

From figure 2, for certain values of all other parameters, it is seen that the absolute value of temperature rises with an increase in the parameter P. The parameter P's influence becomes most noticeable from x=0.2 to 0.5. This may be understood to mean that when the value of P grows (i.e. momentum diffusivity dominates over thermal diffusivity) at a certain cross section, the temperature rises at that cross section. Figure 3 further shows that the magnitude of temperature increases for various levels of E. Figure 4 shows that for a certain cross section (x=0.4), an increase in Reynolds number value has

no effect on temperature change. As inertial forces prevail over viscous forces at the intake, temperature decreases and rises in absolute value, while downstream, temperature turns positive and rises. This may be due to the presence of peristalsis. At the starting cross section (x= 0), the temperature is positive and oscillating, but downstream, the temperature rises as the wave's amplitude grows across the mean half-width of the channel. (Figure 5). According to Figure 6, the temperature for convergent and divergent channels at the inlet is essentially the same as for straight channels. In comparison to its value for a straight channel, the temperature downstream for a divergent channel (K > 0) is greater, but it is lower for a convergent channel (K< 0) in absolute terms towards the boundary. Fig. 7 shows the impact of delta on temperature. As delta varies from 0 to 0.1, it can be observed that the temperature drops, but as delta varies from 0.1 to 0.3, it rises in absolute terms. As the delta value grows, the temperature rises downstream. Peristalsis could be the reason for this.

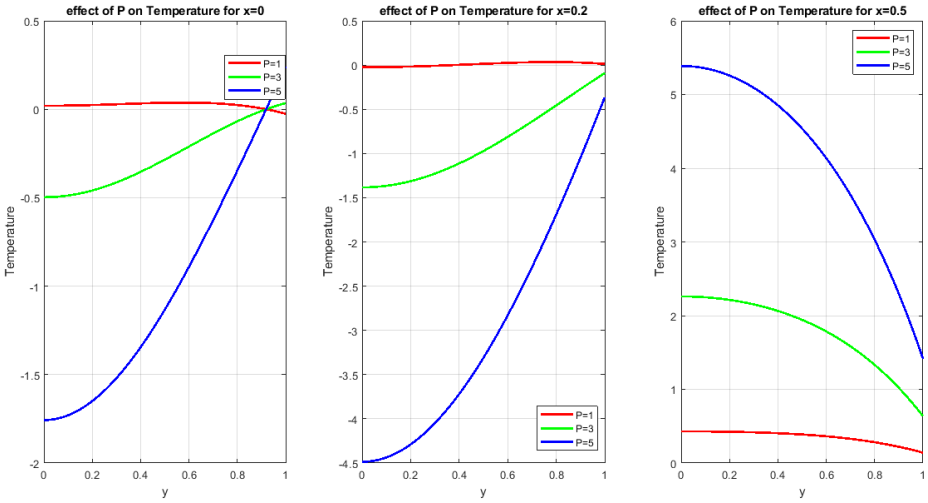

Figure 2. Prandtl number's(P) impact on temperature

(For E = 3,R = 5, δ = 0.1,ε = 0.1, K = 0.1, t = 0.4)

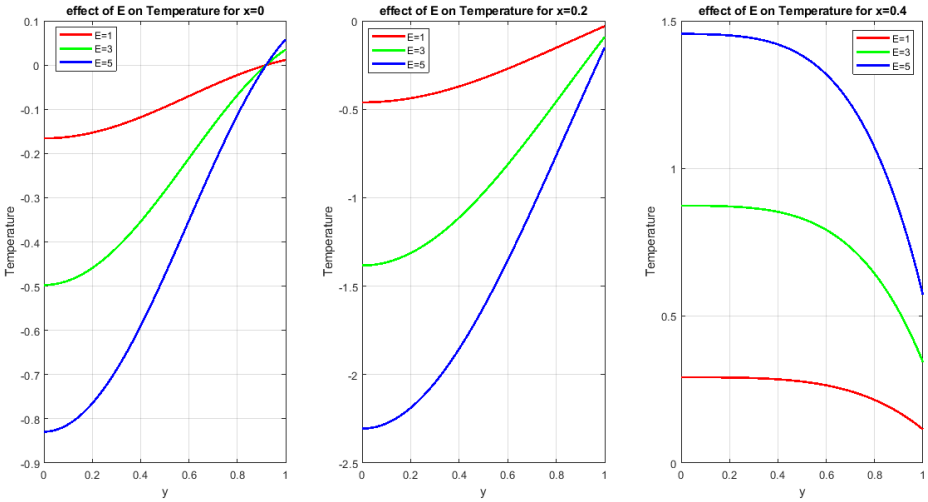

Figure 3. Eckert number's(E) impact on temperature

(For P = 3,R = 5, δ = 0.1,ε = 0.1, K = 0.1, t = 0.4)

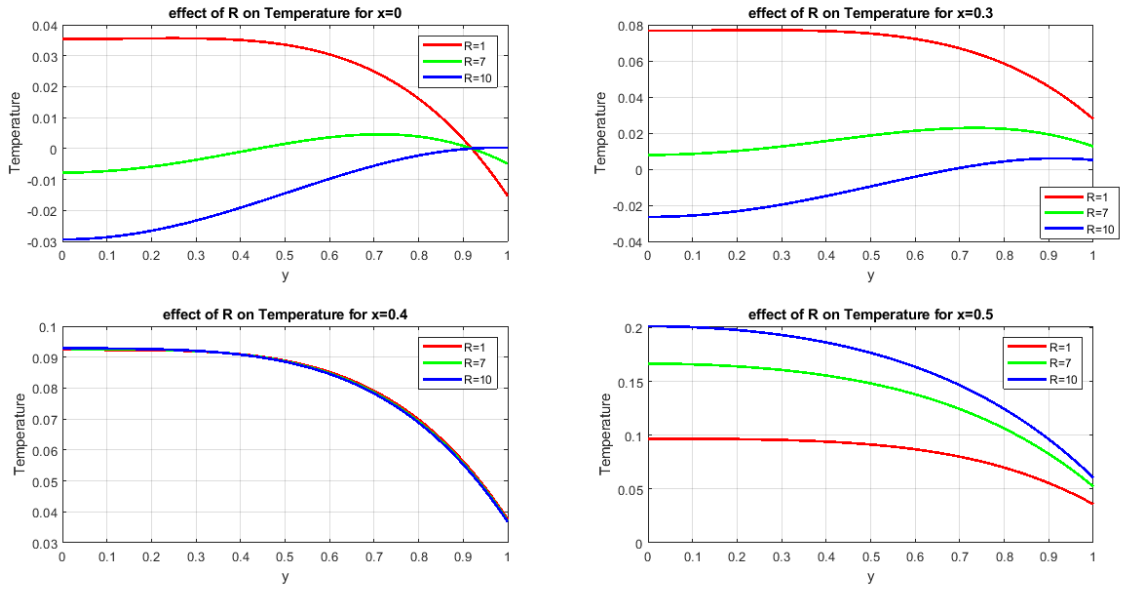

Figure 4. Reynolds number's(R) impact on temperature

(For P = 1,E = 1, δ = 0.1,ε = 0.1, K = 0.1, t = 0.4)

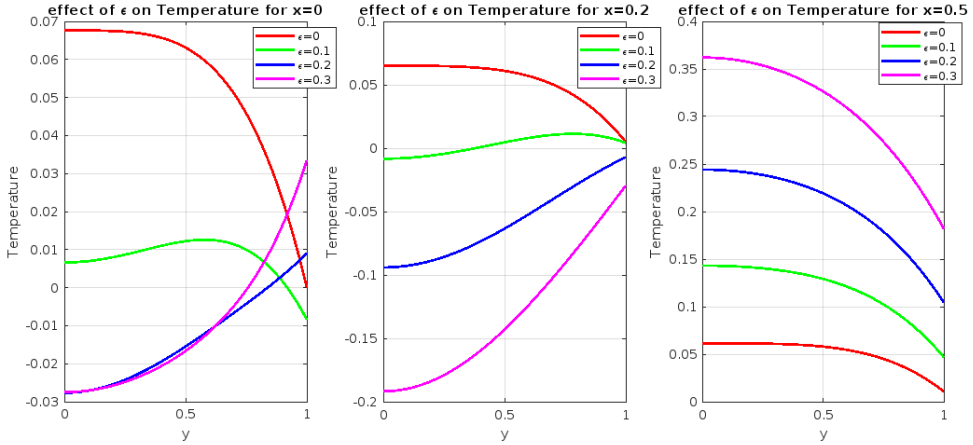

Figure 5. amplitude ratio's(ε) impact on temperature

For P = 1,E = 1, R = 5, δ = 0.1, K = 0.1, t = 0.4)

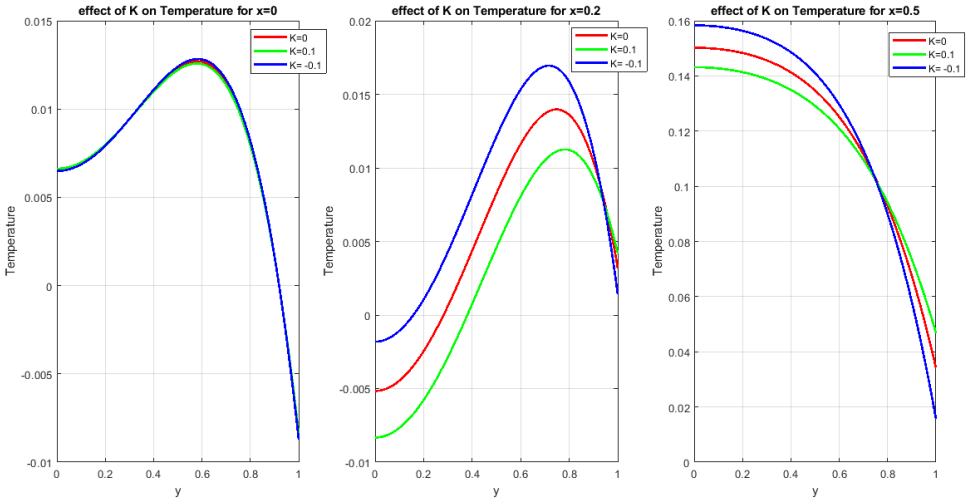

Figure 6. Impact of 'K' on temperature

For P = 1,E = 1, R = 5, ε=0.1, δ = 0.1, t = 0.4)

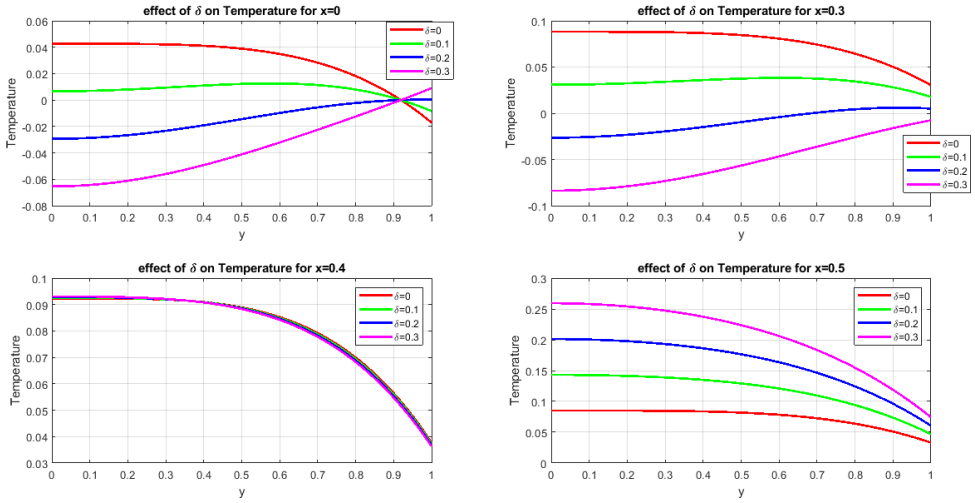

Figure 7. Wall slope's(δ) impact on temperature

For P = 1,E = 1, R = 5, ε=0.1, K = 0.1, t = 0.4)

The information supplied in Tables 1 through 6 makes it clear how different factors affect heat transfer, Z. C_0 is likewise assumed to be '− 0.15' in this instance.

	P				
x	1	2	3	4	5
0	-0.1454	-0.0632	0.2467	0.7844	1.5497
0.2	-0.0914	0.3831	1.4236	3.03	5.2023
0.4	-0.0613	-0.1243	-0.189	-0.255	-0.323
0.6	0.4774	1.3409	2.5904	4.2261	6.2479
0.8	0.1779	0.4657	0.8634	1.3709	1.9883

Table 1. Z variation with P **(For E = 3, R = 5, δ = 0.1, ε = 0.1, K = 0.1, t = 0.4)**

	E				
x	1	2	3	4	5
0	0.0822	0.1645	0.2467	0.329	0.4112
0.2	0.4745	0.949	1.4236	1.8981	2.3726
0.4	-0.063	-0.126	-0.189	-0.2521	-0.315
0.6	0.8635	1.727	2.5904	3.4539	4.3174
0.8	0.2878	0.5756	0.8634	1.1512	1.439

Table 2. Z variation with E **(For P = 3, R = 5, δ = 0.1, ε = 0.1, K = 0.1, t = 0.4)**

	R				
x	1	3	5	7	9
0	-0.699	-0.2262	0.2467	0.7196	1.1925
0.2	-0.8015	0.311	1.4236	2.5361	3.6486
0.6	1.1129	1.8517	2.5904	3.3292	4.068
0.8	0.4256	0.6445	0.8634	1.0823	1.3012

Table 3. Z variation with R **(For P = 3, E = 3, δ = 0.1, ε = 0.1, K = 0.1, t = 0.4)**

	ε		
x	0	0.1	0.2
0	-0.2193	0.2467	2.5809
0.2	-0.1964	1.4236	7.8493
0.6	-0.1585	2.5904	9.8232
0.8	-0.1428	0.8634	2.7654

Table 4. Z variation with ε **(For P = 3, E = 3, R = 5, δ = 0.1, K = 0.1, t = 0.4)**

	K		
x	-0.1	0	0.1
0	0.1171	0.1814	0.2467
0.2	0.9381	1.1841	1.4236
0.4	0.2767	0	-0.1891
0.6	5.5488	3.8031	2.5904
0.8	3.1622	1.6759	0.8634

Table 5. Z variation with K **(For P = 3, E = 3, R = 5, δ = 0.1, *ε* = 0.1, t = 0.4)**

	δ		
x	0	0.1	0.2
0	-1.0091	0.2467	1.5026
0.2	-1.531	1.4236	4.3781
0.6	0.8728	2.5904	4.3081
0.8	0.351	0.8634	1.3758

Table 6. Z variation with δ **(For P = 3, E = 3, R = 5, ε = 0.1, *K* = 0.1, t = 0.4)**

Using table 1, Z seems negative for certain values of P and turns positive for other values of P. As P rises, the values of Z also rise. Table 2 makes it clear that at the entry, heat transfer is positive and rises

with E. For x=0 to 0.4, the value of Z's rise and fall is the same as what is seen downstream. Using table 3, Heat transfer is found to be negative for some values of R, but it is positive downstream and rises with R. Tables 4-6 demonstrate how geometric factors affect heat transmission. According to Table 4's data, Z is always negative for all values of x ($\varepsilon = 0$), but it gradually turns positive and rises as ε rises. For x=0 to x=0.2, value of Z decreases for convergent channels and increases for divergent channels. However, the value of Z grows for convergent channels and reduces for divergent channels downstream (Table 5). Heat transfer turns negative for some values of δ, as seen in Table 6, but as δ rises, its absolute value increases.

The value of the heat transfer coefficient rises by an average of 18 to 21% for certain values of specific characteristics. The information from the current investigation will be instrumental in the nuclear industry, the development of smart magneto-peristaltic pumps, and creating interest among young researchers to concentrate on the wall effects of different types of Newtonian fluids in the presence of peristalsis.

References

[1] Shapiro AH, Jaffrin MY, and Weinberg SL, Peristaltic pumping with long wavelengths at low Reynolds number, *Journal of Fluid Mechanics*. 1969; 37: 799-825.
[2] Zien TF, Ostrach S, A long wave approximation to peristaltic motion, *Journal of Biomechanics*. 1970; 3: 63-75.
[3] Walker SW, Shelley MJ, Shape optimization of peristaltic pumping, *Journal of Computational Physics*. 2010; 229: 1260-1291.
[4] Srinivas ANS, Reganti, Hemadri Reddy, Srinivas S, Sreenadh S, Peristaltic transport of a Casson fluid in a channel with permeable walls. International Journal of Pure and Applied Mathematics, 2014, 90. 10.12732/ijpam.v90i1.3.
[5] Kavitha A, Hemadri Reddy R, Saravana R, Sreenadh S, Peristaltic transport of a Jeffrey fluid in contact with a Newtonian fluid in an inclined channel, Ain Shams Engineering Journal, 2017, 8(4), 683-687,ISSN 2090-4479, Available from https://doi.org/10.1016/j.asej.2015.10.014.
[6] Prasad KV, Vajravelu K, Hanumesh Vaidya, Neelufer Z. Basha, Umesh V,Thermal and species concentration of MHD Casson fluid at a vertical sheet in the presence variable fluid properties, Ain Shams Engineering Journal, 2018, 9(4), 1763-1779, ISSN 2090-4479. Available from https://doi.org/10.1016/j.asej.2016.08.017.
[7] Saravana R, Vajravelu K, Sreenadh S,Influence of Compliant Walls and Heat Transfer on the Peristaltic Transport of a Rabinowitsch Fluid in an Inclined Channel" *Zeitschrift für Naturforschung A*, 2018, 73(9), 833-843. Available from https://doi.org/10.1515/zna-2018-0181.
[8] Ashmawy EA, Effects of surface roughness on a couple stress fluid flow through corrugated tube, *European Journal of Mechanics-B/Fluids.* 2019; 76: 365-374.
[9] Devaki P, Kavitha A, Venkateswarlu Naidu D, Sreenadh S, The Influence of Wall Properties on the Peristaltic Pumping of a Casson Fluid. Trends in Mathematics. Birkhäuser, Cham, 2019. Available from https://doi.org/10.1007/978-3-030-01123-9_18.
[10] Divya BB, Manjunatha G, Rajashekhar C, Hanumesh Vaidya, Prasad KV,Analysis of temperature dependent properties of a peristaltic MHD flow in a non-uniform channel: A Casson fluid model, Ain Shams Engineering Journal, 2021;12(2) ,2181-2191,ISSN 2090-4479, Available from: https://doi.org/10.1016/j.asej.2020.11.010.
[11] Alhazmi SE, Imran A, Awais M, Abbas M, Alhejaili W, Hamam H, Alhowaity A, Waheed, A. Thermal convection in nanofluids for peristaltic flow in a nonuniform channel. Sci Rep. 2022 Jul 25;12(1):12656.
[12] Varahadpande IG, Murty VRK, Sekhar PS, Oscillatory Flow of Dusty Fluid Through a Narrowed Channel in the Presence of Magnetic Field, Recent Advances in Applied Mathematics and Applications to the Dynamics of Fluid Flows. *Lecture Notes in Mechanical Engineering.* 2022; 63-76. doi: 10.1007/978-981-19-1929-9.
[13] Bhattacharyya A, Kumar R, Bahadur S, Seth G S, Sunil, Modeling and interpretation of peristaltic transport of Eyring–Powell fluid through uniform/non-uniform channel with Joule heating and wall flexibility, Chinese Journal of Physics, 2022; 80, 167-182,ISSN 0577-9073. Available from: https://doi.org/10.1016/j.cjph.2022.06.018.
[14] Ammar N, Ali H, Mathematical modelling for peristaltic transport of non-newtonian fluid through inclined non-uniform channel under the effect of surface roughness. International Journal of Nonlinear Analysis and Applications, 2022; 13(2), 117-130. doi: 10.22075/ijnaa.2022.27621.3671.